Journal of Applied Electrochemistry **33**: 465–473, 2003.

Electropolymerization of aniline on carbonized polyacrylonitrile aerogel electrodes: applications for supercapacitors

H. TALBI, P.-E. JUST and L.H. DAO*
Advanced Materials Research Laboratory, INRS-Energy-Materials-Telecommunication, University of Québec, 1650 Blvd Lionel-Boulet, Varennes, Qué, Canada, J3X 1S2
*(*author for correspondence, e-mail: dao@inrs-emt.uquebec.ca)*

Received 28 September 2002; accepted in revised form 25 February 2003

Key words: carbon aerogel, conducting polymer, polyacrylonitrile, polyaniline, supercapacitor

Abstract

Polyaniline was electrochemically synthesized on carbon polyacrylonitrile aerogel electrodes for use as active material in supercapacitor devices. Electrochemical characterization was performed by cyclic voltammetry, electrochemical impedance spectroscopy (EIS) and charge–discharge experiments in aqueous medium. Two types of electrochemical phenomenon were observed; the first is based on electrostatic energy storage in the double layer at the interface solution/carbon polyacrylonitrile (PAN) aerogel, the other is associated with the redox processes in polyaniline, for which the faradaic charge depends on the potential range. The performance of the supercapacitor was tested for capacity, energy and power density and self-discharge. Specific capacitance as high as 230 F g^{-1} was reached. A symmetrical supercapacitor showed good cyclability (over 3000 cycles) during repeated charge–discharge cycles. The results are very promising and demonstrate the viability of a symmetric supercapacitor based on carbon PAN aerogel covered by an electronically conducting polymer.

1. Introduction

Electrochemical supercapacitors are energy storage devices, similar to batteries, but with much higher power density [1, 2]. These devices are based either on the double-layer capacitance of electrode materials with high surface area or on a redox pseudocapacitance of faradaic-active materials. The growing interest in these devices is stimulated by their potential applications in high power equipment such as electric vehicles [2, 3], cellular phones and other applications requiring fast charge–discharge ability [2].

On the one hand, preparation of highly porous electrodes based on polyacrylonitrile aerogel has been achieved recently [4, 5]. A direct application of such porous electrodes is found in electrochemical double-layer supercapacitors [5]. On the other hand, electronically conducting polymers (ECP) have been also used as supercapacitor electrodes [2, 6, 7] in which energy is stored by the reversible electrochemical doping-undoping reaction. Specific power delivered by carbon/carbon supercapacitors can reach 3 kW kg^{-1}, with maximum specific energies of 5 Wh kg^{-1}. The conventional conducting polymer-based supercapacitors can reach specific power values of 2 kW kg^{-1} with a specific energy of more than 10 Wh kg^{-1} [2]. In this last case, the capacity is determined entirely by the electrochemical redox reaction of the π-conjugated system.

To increase the specific capacity of the PAN aerogel-based supercapacitors, we have been attempting to combine the capacitance of the double layer with the redox reaction of the π-conjugated system. A cooperative effect of a π-conjugated system of a relatively high specific capacity with a porous PAN-aerogel system should give even larger specific capacity than just the porous system or the conducting polymer alone. As an example of this combination, we propose to cover the porous structure of PAN aerogel previously deposited onto carbon paper, with a thin film of polyaniline. The redox mechanism will involve both the formation of double layer into the porous structure of the PAN aerogel and the p-doping of the π-conjugated polymer, both reactions occurring at the same potential. Of all the p-doping conducting polymers, polyaniline appears to be a particularly attractive material because of its high electroactivity, high doping level [8] and excellent stability [9–11]. Polyaniline have been widely studied for use in lithium batteries [12–14] and in electrochemical supercapacitors [2, 15–17]. It can give specific capacitance in the range of 400 to 500 F g^{-1} in aqueous acidic medium [2].

In this study, we discuss the properties of PAN aerogel electrochemically covered with a thin film of polyaniline as electrode material in supercapacitor devices. The performances of the PANCF-PANI/PANI-PANCF electrochemical supercapacitor were

evaluated using the following techniques: cyclic voltammetry, charge–discharge cycles and impedance (EIS). The supercapacitor self-discharge was also examined.

2. Experimental details

All chemicals were purchased from Aldrich and used without further purification (aniline > 99.5%, H_2SO_4 95–98%, ACS reagents).

2.1. *Fabrication of electrodes*

Polyacrylonitrile (PAN) aerogel was deposited onto the carbon paper using a procedure described elsewhere [5]. Briefly, PAN aerogel is prepared from a solution consisting of 5 g of polyacrylonitrile in a 100 dm^3 mixture of dimethylformamide (DMF): water (84:16 v:v). The resulting solution was stirred vigorously and heated to ~135 °C until the complete dissolution of PAN. Carbon paper sheets Technimat 6100-035 purchased from Lydall Technical Papers were dipped into the boiling solution, then soaked in acetone prior to the pretreatment and carbonization processes. The pretreatment process was performed in air at 215 °C for 20 h, followed by a carbonization step performed at 850 °C for 8 h in an inert atmosphere (Argon), leading to the starting material named PANCF.

2.2. *Electrochemical studies*

All electrochemical experiments were performed using an EG&G galvanostat–potentiostat (model 273). The electrochemical impedance measurements were carried out using a Solartron HF response analyser (model 1255). A 10 mV amplitude sinusoidal signal was applied, from 100 kHz to 10 mHz, 8 points per decade change in frequency.

The electropolymerization was performed in a three-electrode cell, using an 0.1 M aniline and 1 M H_2SO_4 aqueous solution. The working electrodes were 0.8 cm × 2 cm and 0.035 in thick fibre carbon paper with surface area of 1–2 $m^2\ g^{-1}$. Platinum wire was used as counter electrode. The reference electrode was a typical Ag/AgCl. The as-formed films were removed from the growth solution, washed in distilled water to remove any soluble species from the film and then cycled in a 1 M H_2SO_4 monomer free solution.

The electrochemical cell in the symmetrical supercapacitor geometry for the cyclic voltammetry and the chronopotentiometric studies was a two-electrode set-up in aqueous 1 M H_2SO_4. The two electrodes were separated by a filter paper previously soaked with the 1 M H_2SO_4 electrolyte. For this two-electrode cell, the electrode area was 1 cm^2. The chrono-potentiometric studies of galvanostatic charge–discharge cycles were carried out in the potential range 0 to 0.6 V. For calculation of the energy and power densities, the first discharge curve after equilibration of the cell at 0.6 V was considered, and the total dry mass of the polymeric material (PAN aerogel and PANI) of the two electrodes was taken into account.

SEM of the PANCF and the PANI/PANCF electrodes was performed using a Jeol apparatus at 5 keV.

3. Results and discussion

3.1. *Electrochemical synthesis of polyaniline onto PANCF*

Figure 1 shows the cyclic voltammograms of aniline in 1 M H_2SO_4 onto PANCF (polyacrylonitrile aerogel deposited on the carbon paper), using repeated potential scans between 0 and 1 V vs Ag/AgCl. The first scan shows an irreversible anodic peak corresponding to the oxidation of aniline at $E_a = 0.76$ V vs Ag/AgCl. This peak disappears during the second cycle and a new peak attributed to the oxidation of the as-formed polyaniline (PANI) appears at around 0.5 V. On the return scan is observed a peak at 0.28 V corresponding to the reduction of the thin PANI film. Continuous cycling results in an increase of the current of the oxidation and reduction waves, corresponding to the continuous growth of the polymer at the electrode. Similar features for the oxidation of aniline have been observed on the platinum electrode.

Polyaniline can also be deposited potentiostatically on the PANCF surface. The potentiostatic experiments were carried out at 1.0 V for different times: 2, 5, 10, 20, 35 and 50 s in order to determine the required time needed to promote the formation of a thin film into the pores of the carbonized PAN aerogel.

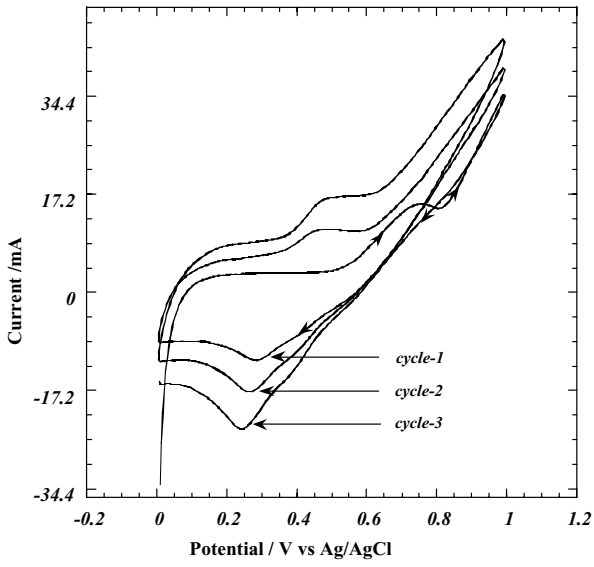

Fig. 1. Electrochemical oxidation of aniline on a carbon paper covered with PAN aerogel electrode. Scan rate 20 mV s^{-1}. Medium: 1 M H_2SO_4.

3.2. *SEM characterization*

Photomicrographs were obtained for the 'raw' and for the PANI covered carbonized PANCF electrodes. The micrographs of the pristine material show a homogeneously dispersed polyacrylonitrile on the surface of the carbon paper under lower magnification (Figure 2(a)). The carbon fibres appear to act as anchors for the polymer, which is located between the fibres rather than on them. Only a very thin inhomogeneous film of PAN is deposited onto the carbon fibres. Higher magnifications (Figure 2(b) and (c)) of the PAN aerogel surface show a highly porous structure easily accessible to the electrolyte. This carbonized material looks like a foam with a highly reticulated structure. Similar morphology have been previously observed in our laboratory, when this material is dried by supercritical CO_2 or prepared by inverse emulsion [4, 18]. Deep pores of large diameters are observed, which is consistent with the hydrogel-like structure of this material, but which prevents the formation of a double layer. Indeed, only a pore diameter in the range or lower than 50 nm is beneficial for the charge accumulation and so, for the formation of a double layer.

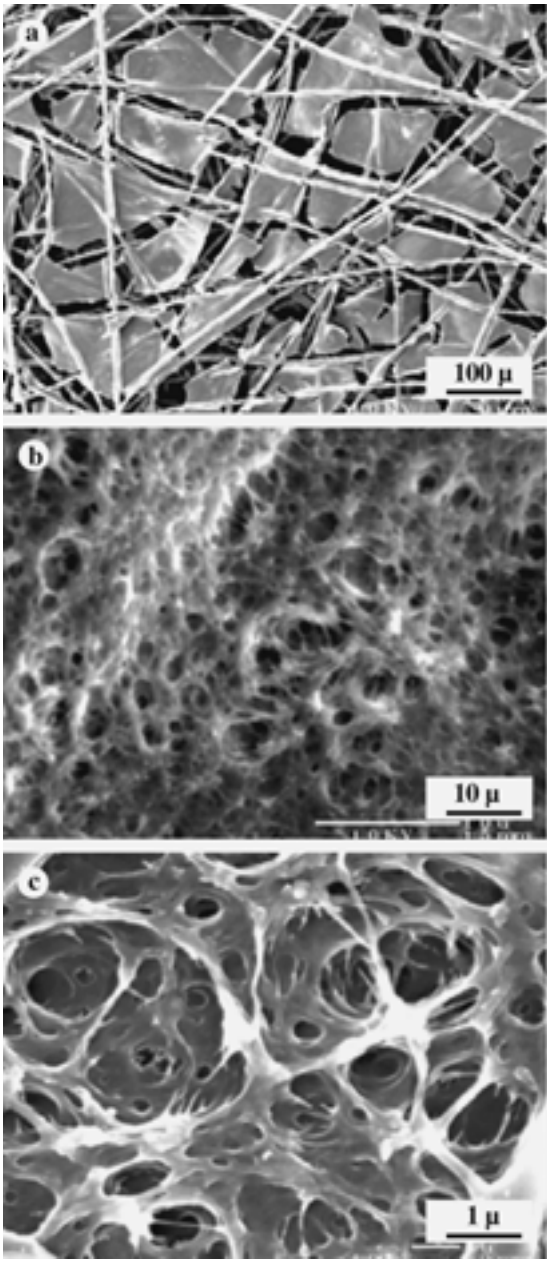

Fig. 2. SEM photomicrographs of PAN aerogel deposited onto carbon paper. SEMs recorded at different magnifications: (a) ×100, (b) ×3000, (c) ×10 000.

In an effort to understand the differences in electrochemical responses described thereafter, SEM photomicrographs were taken for the PANCF covered with polyaniline film for different electropolymerization times. We focus here on the samples obtained for a growing time of 20 s. In this case, SEM shows the formation of a disordered and tangled PANI fibrous structure (Figure 3(b) and (c)) which covers unhomogeneously the PANCF surface. The electropolymerization takes place into the porous structure and covers the major part of the PANCF surface. This probably induces an increase of the specific surface area. The SEMs taken for the growing surface of the PANI films (Figure 3(c)) are in agreement with those previously obtained for polyaniline grown in aqueous and organic solvents, which show a fibrous morphology [19, 20]. Figure 3(d) shows the morphology of PANI deposited onto carbon fibre for the same deposition time (i.e., 20 s). The structure of the PANI is similar to that described before and the deposition time used is not sufficient to give a homogeneous surface onto the carbon fibre used as substrate. Deposition times higher than 20 s lead to the formation of a relatively thick film which covers the whole surface of the PAN aerogel and carbon paper. This induces a disappearance of the electrochemical response of the PAN aerogel as discussed below.

3.3. *Electrochemical studies of PANCF/PANI electrodes*

3.3.1. *Electrochemical behaviour in a three-electrode cell*

The PANCF/PANI electrodes obtained at different deposition times were cycled between −0.3 and 0.7 V (Figure 4). The 'raw' PANCF electrode, without PANI film, presents a square signal related to the double layer capacitative behaviour [4, 5]. For the electrodes covered with PANI obtained for deposition time of 2 s and 5 s, it appears two redox processes, at $E_a = 0.17$ V and $E_a = 0.43$ V, related to the p-doping of the PANI. For deposition times higher than 20 s, the square signal of PANCF (Carbon fibre covered with PAN) is strongly reduced and the peaks related to the electrochemical behaviour of PANI are predominant. The film of PANI formed in this case covers the whole surface of the porous PAN aerogel material and prevents the charge accumulation into the pores and the formation of the double layer. Deposition time of 20 s seems to be more convenient to preserve the double layer capacitive behaviour of the PAN aerogel material.

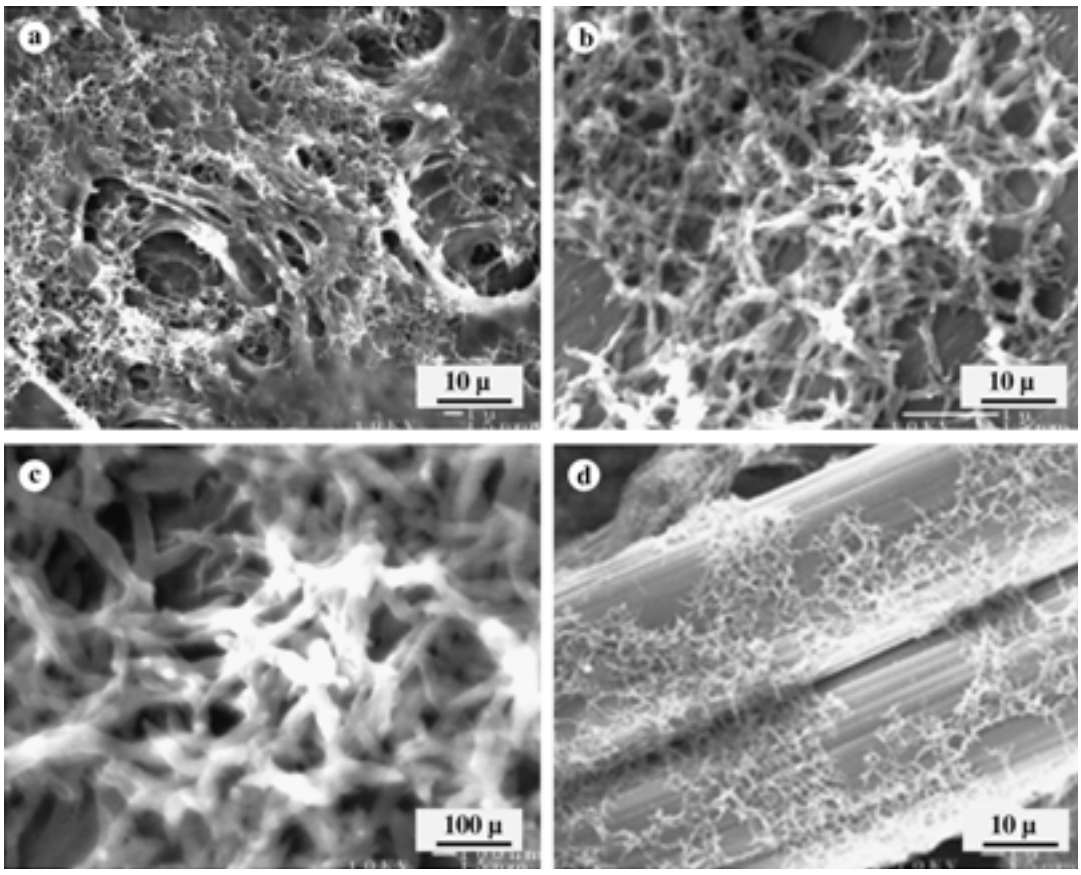

Fig. 3. SEM photomicrographs of polyaniline deposited onto PANCF electrodes. Deposition time: 20 s. Different magnifications: (a) ×4000, (b) ×20 000, (c) ×50 000, (d) ×5000.

The CVs recorded at three different potential scan rates are presented in Figure 5. CVs of PANI deposited during 20 s onto carbon paper (Figure 5(a)) are characterized by two sets of major waves. Between −0.3 and 0 V, the current is lower than 0 mA. Such behaviour is not observed in the case of PANI deposited during the same time onto PANCF (Figure 5(b)). In this case, the anodic current intensity is very important and a square signal is clearly observed between −0.3 to 0 V. This indicates that the electrochemical response of the composite PANCF/PANI is a combination of two different phenomena: the electrochemical capacitive behaviour of PAN aerogel and the I/E response of the PANI.

Generally thick films peel off from the electrode; this did not happen with the PANCF electrodes due to good adhesion of the polymer film on the electrode. To investigate more deeply the electrochemical behaviour of polyaniline on the carbon PANCF electrode, a platinum electrode was used to perform a comparative study of the potentiostatic electrooxidation of aniline at the two electrodes for the same duration. The charge in coulomb passed for the film formation and the charge passed for the complete oxidation of the as formed film of PANI are gathered in Table 1. The PANCF electrode consumes more charge than the platinum electrode, probably because of its great effective and porous surface area. Table 1 indicates also that films formed on the PANCF electrodes produce higher peak current densities I_a than films obtained on platinum. The oxidation of aniline and the doping of PANI occur on the surface of the PANCF and also inside the porous structure of the carbonized PAN aerogel.

The peak potential for the PANI film oxidation is shifted, due to the adsorption of the polymer in these pores. It is also possible that the polymer formed in the pores has a more conjugated structure. In Table 1, the efficiency ε is defined as the charge passed for the conversion of PANI (Q_c) from the fully reduced state ($E = -0.3$ V) to the fully oxidized state (0.7 V) reported to the charge consumed during the formation of PANI (Q_s). The values of efficiency indicate that the PANCF produces more polyaniline by oxidation of aniline than platinum does. This behaviour could be explained by the confinement of the reaction in the pores in which aniline diffuses. Oxidation of aniline generates cation radicals, which remain in confined spaces for effective polymerization.

Voltammograms recorded with PANI–PANCF electrodes show large background currents (Figure 4). This current increases with increasing the sweep rate, suggesting that it is a capacitive current. The voltammetric curves at $E = 0$ V vs Ag/AgCl and beyond the decay of faradaic current ($E = 0.55$ V) were analysed to deter-

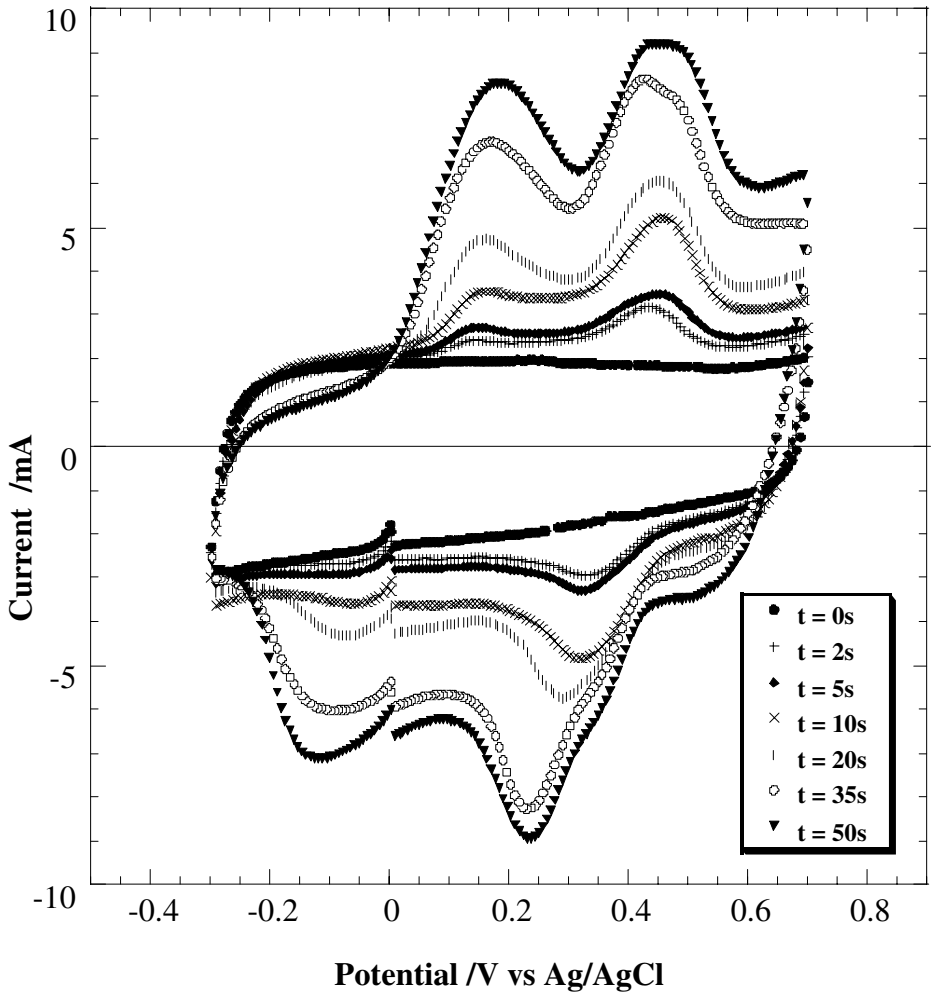

Fig. 4. Cyclic voltammogram of PANCF covered with PANI as conducting polymer. Scan rate: 20 mV s^{-1}. Medium 1 M H_2SO_4. Electrodes are obtained for different deposition times ($t = 0$ s to 50 s).

mine the specific capacitance values. The following equation was used:

$$C = \frac{1}{2m}\left(\frac{dI}{d\nu}\right) \quad (1)$$

where C is the specific capacitance (in F g^{-1}), I the sum of the anodic and cathodic currents, v the potential scan rate and m the weight of active material (PAN aerogel and polyaniline) (in g). The specific capacitance values obtained are presented on Table 2. The capacitance increases with increasing the PANI deposition time. A capacitance value as high as 207 F g^{-1} is reached when PANI is deposited onto the PANCF during 35 s. This value could be the sum of the double-layer capacitance of the carbonized PAN aerogel and the pseudocapacitance of the PANI film. The specific capacitance is increasing with the deposition time of polyaniline onto PAN aerogel and is maximized at a deposition time of 50 s (Figure 6). This indicates that the deposition time of 50 s is sufficient to cover the entire PANCF electrode surface. Thus, the apparent specific capacitance measured is related only to the pseudo-capacitance of polyaniline. Specific capacitance as high as 240 F g^{-1} is reached in the case of sample obtained after 100 s. Note that polyaniline can give specific capacitance in the range 400 to 500 F g^{-1} in aqueous acidic medium [2]. This value is reachable in our case for deposition time higher than 50 s if we take into account only the mass of polyaniline.

3.3.2. *Electrochemical studies in 2-symmetrical supercapacitor geometry*

Cyclic voltammograms recorded with PANCF-PANI electrodes in 2-symmetrical supercapacitor geometry in 1 M H_2SO_4 aqueous electrolyte are shown in Figure 7. Their shape approaches the ideal rectangular form characteristic of a capacitance independent of the applied potential, with several oxidation and reduction waves, which is characteristic of pseudo-capacitance behaviour in conducting polymers. Our behaviour is closely similar to that of Ruthenium oxides (RuO_2) [21] for which the cyclic voltammogramms approach the ideal rectangular shape expected for a regular capacitor. The capacitor geometry studied here corresponds to type I electrochemical capacitor, both electrodes being based on conducting polymers of the p-dopable type, that is, with oxidation leading to positively charged

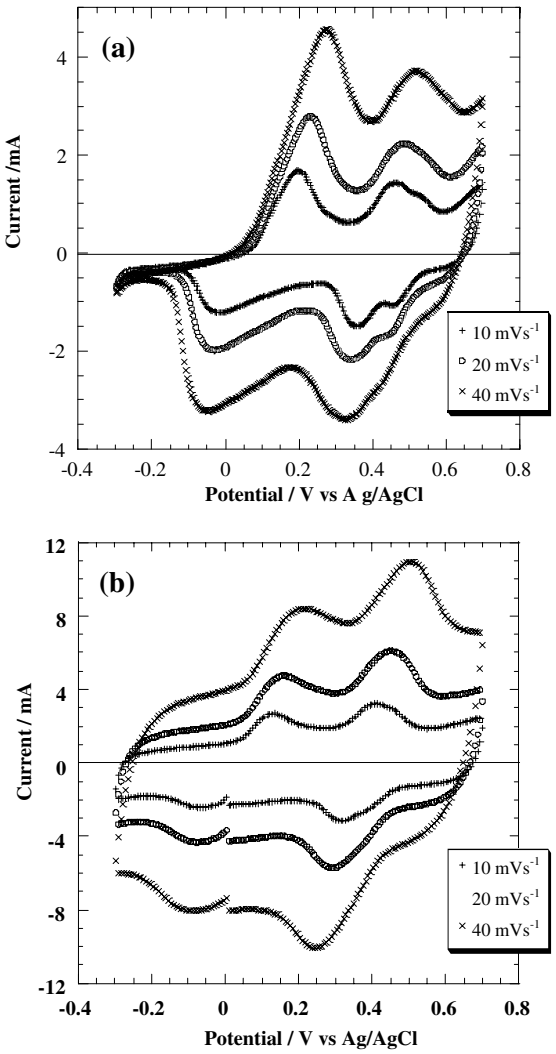

Fig. 5. Electrochemical response of PANI deposited onto carbon paper (a) and onto carbonized PAN aerogel (b) at different sweep rates. Deposition time 20 s at 1 V vs Ag/AgCl.

Table 1. Charges quantity passed for the formation of polyaniline on a carbon PANCF electrode and on a platinum electrode in the potentiostatic mode. Q_c and I_a are determined from the CVs recorded at a scan rate 20 mV s^{-1}. Medium: 1 M H_2SO_4

Duration /s	Q_s /mC	Q_c /mC	Efficiency $\varepsilon = Q_s/Q_c$	I_a /mA
PANCF working electrode				
2	80.6	46.74	0.58	3.19
5	115.7	60.16	0.52	3.45
10	317.0	148.77	0.47	5.22
20	503.3	169.91	0.38	6.10
35	1057.4	296.07	0.28	8.40
Platinum working electrode				
5	66.0	13.86	0.21	0.11
10	95.2	17.13	0.18	0.17
20	133.1	22.63	0.17	0.26
35	291.2	43.68	0.15	1.05

polymers chains. In the fully charged state, one electrode will be in the uncharged state and the other in the fully p-doped state. A potential of 0.7 V will become established between the electrodes, with half this range being available for capacitor charge and discharge processes.

Table 2. Specific capacitance calculated at $E = 0$ V vs Ag/AgCl for different deposition times, in three-electrode cell configuration

Oxidation time /s	Specific capacitance/F g^{-1} calculated at $E = 0$ V	Specific capacitance/F g^{-1} calculated at $E = 0.55$ V
0	85.27	62.46
2	87.41	65.08
5	91.28	76.90
10	118.23	93.00
20	136.29	118.65
35	207.69	198.12
50	232.60	207.40

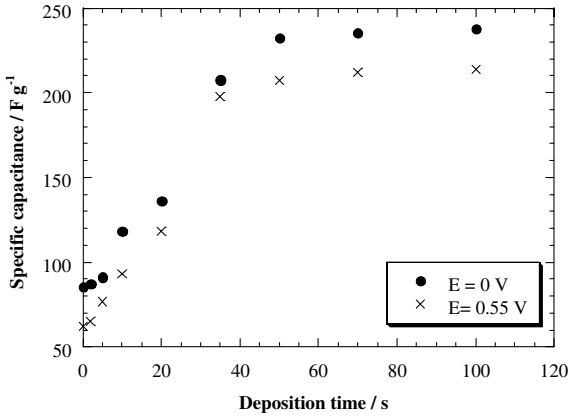

Fig. 6. Variation of the specific capacitance with the deposition time of polyaniline. Key: (●) $E = 0$ V and (×) $E = 0.55$ V.

The specific capacitance values were calculated using Equation 1, considering anode and cathode as active materials, not including the electrolyte. The results are gathered in Table 3. Here again, the capacitance increases with increasing the PANI deposition time. Specific capacitance as high as 38.9 F g^{-1} is obtained for a deposition time of 35 s. The specific capacitance values obtained in a two-electrode cell confirm the fact that the capacitance measured in 2-symmetrical supercapacitor geometry corresponds roughly to one-quarter of the value calculated in a three-electrode cell (half cell or individual electrode) [22, 23].

Figure 8 displays the galvanostatic charge–discharge cycle of the supercapacitor between 0 V and a maximum cell voltage of 0.6 V at a constant current density of 1 mA. The supercapacitor was charged from 0 to 0.6 V and then discharged from 0.6 to 0 V, coulombic efficiency near 100% being obtained. In Figure 9, the variation of the discharge capacity with repeated charge–discharge cycles at a current density of 5 mA is displayed. Whatever the deposition time, all the samples exhibit roughly similar behaviour. An irreversible faradaic reaction occurs during the first charge–discharge cycles. For the sample obtained at a deposition time of 20 s, 15.3% of the charge capacity is irreversibly consumed by this reaction. Such deterioration is more

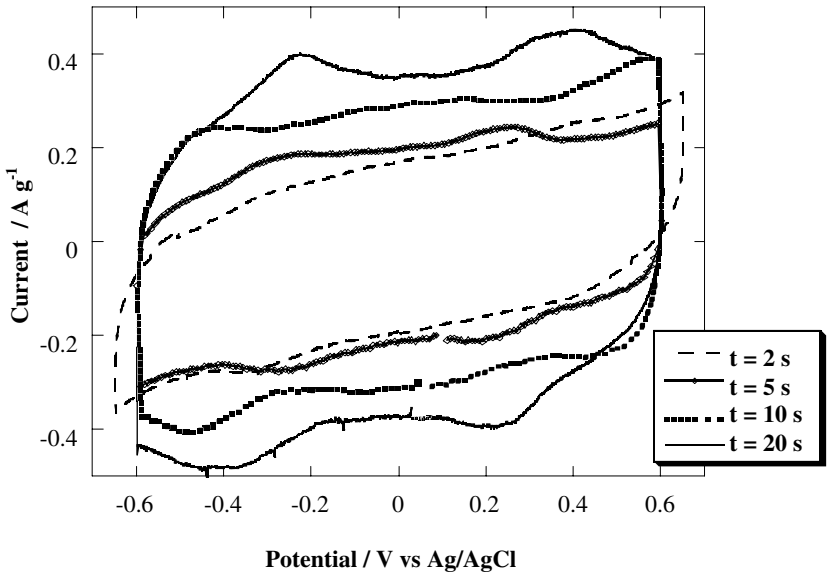

Fig. 7. Cyclic voltammograms recorded in 2-symmetrical supercapacitor cells based on PANCF–PANI electrodes obtained for different deposition times. Scan rate 10 mV s^{-1}. Medium: 1 M H_2SO_4.

Table 3. Specific capacitance calculated for different deposition times, in 2-symmetrical supercapacitor configuration

Oxidation time /s	Specific capacitance/F g^{-1} calculated at $E = 0$ V
2	19.56
5	21.48
10	30.32
20	35.55
35	38.92
50	40.83

Capacitance calculated per gram of active material (i.e., PAN + PANI) on both electrodes in the supercapacitor configuration.

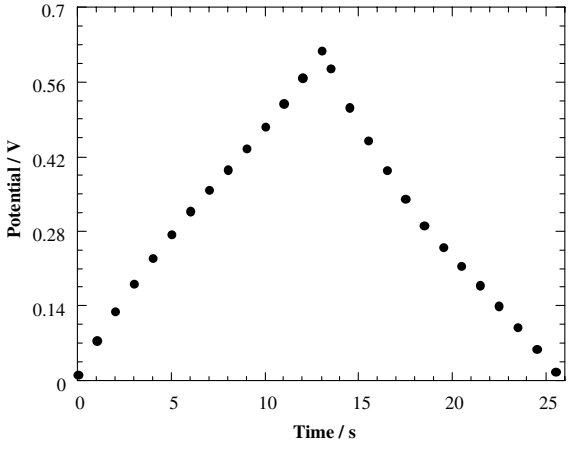

Fig. 8. Charge–discharge cycle between 0 and 0.6 V at 1 mA of PANCF–PANI supercapacitor. PANI deposition time 20 s.

important in the case of samples obtained for a long deposition time ($t \sim 50$ s). It must be noticed that for a supercapacitor based only on carbonized PAN aerogel, no deterioration has been observed in its performance

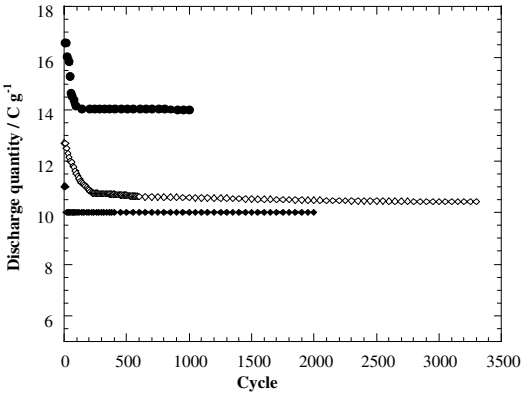

Fig. 9. Cycle life performance of PANCF–PANI based supercapacitor during constant current charge–discharge multicycles at 5 mA between 0 and 0.6 V. PANI onto PAN aerogel deposition times10 s (♦), 20 s (◇) and 50 s (●).

upon a long cycling period (higher than 10^4 cycles) [24]. In our case, such decrease could be related to a kinetic degradation of PANI, which gives rise to the formation of p-aminophenol and p-benzoquinone [25, 26]. An other reason for this decrease could be the formation during the repeating cycles of some degradation products or α–β side-couplings, introducing defects in the polymer chain.

The self-discharge of the PANCF-PANI supercapacitor was also tested, after the cell has been maintained at a constant potential of 0.65 V during 10 min (Figure 10). The system undergoes relatively rapid self discharge in the first few minutes. This self-discharge is quite limited: only 14% of the initial charge was lost after 2 h and at around 20% after 10 h.

The 2-symmetrical capacitor cell was further characterized using impedance measurements. The Nyquist plot is presented in Figure 11. The shape of the

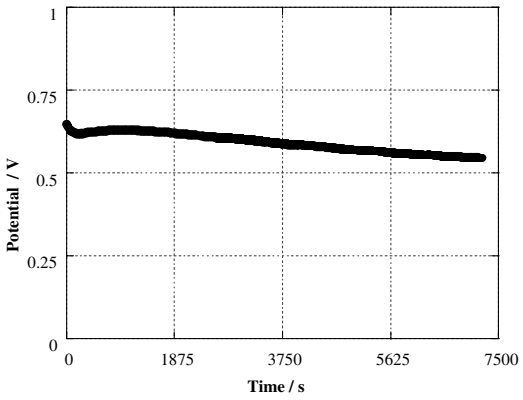

Fig. 10. Self-discharge of PANCF–PANI based supercapacitor. PANI deposition time 20 s.

spectrum is closely similar to those observed in the case of carbon materials and pseudo-capacitive materials such as conducting polymers and noble metal oxide electrodes [27–30]. Three distinct regions are present, dependent of the frequency range. In the low frequency region, the impedance of the cell increases and tends to become purely capacitive (vertical lines characteristic of a limiting diffusion process). In the intermediate frequency region is the 45° line characteristic of ion diffusion into the porous structure of the electrode. At high frequency occurs the charge transfer process. This semicircular region has a relatively small radius of curvature for all the samples studied, which indicates low resistance to the charge transfer process. The sample synthesized for a deposition time of 20 s shows a much larger radius due to the lesser magnitude of the charge transfer in the electrode.

The specific capacitance of the material is obtained at low frequencies (i.e., 1–0.01 Hz region) according to the formula: $|Z''| = 1/2\pi f C_{\mathrm{dl}}$. The linear regression of the plot $Z'' = f(1/f)$ gives a slope equal to $(2\pi C_{\mathrm{dl}})^{-1}$.

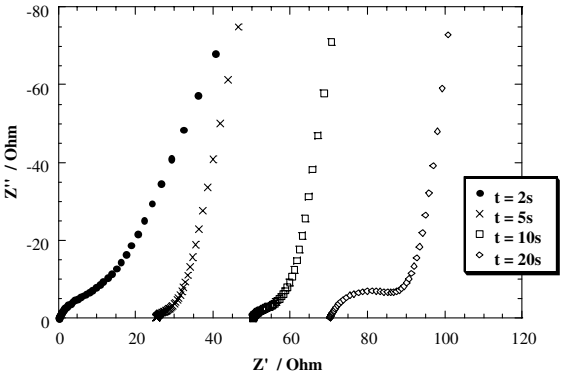

Fig. 11. Impedance spectra in the complex plane of PANCF–PANI-based supercapacitors for different PANI onto PAN aerogel deposition times ($t = 2$ to 20 s). Electrode potential corresponding to the open circuit. Medium 1 M H_2SO_4. Impedance spectra are plotted between 100 kHz and 10 mHz. Curves have been arbitrarily shifted along the abscissa (x-axis) for clarity.

The values obtained are roughly consistent with the capacitance calculated from cyclic voltammetry in the 2-symmetrical supercapacitor geometry. Figure 12 shows a typical plot of the specific capacitance as a function of the frequency for different deposition times of PANI on carbonized PAN aerogel. The best electrodes (deposition time of 20 s) attain a maximum specific capacitance of 34 F g^{-1} in the frequency range useful for load levelling in traction applications.

The performance of the system as supercapacitor was investigated, using its energy density and its charge cycle efficiency. The latter, defined as the ratio of the energy delivered by the supercapacitor upon discharge to the energy needed to charge it, is close to 100% as shown before in Figure 8. The energy output of a supercapacitor is dependent on the power density at which the energy is extracted [31]. The energy and power densities delivered by the supercapacitor were evaluated from the galvanostatic discharge curves by taking into account only the mass of the electroactive material of both electrodes. The specific energy (Wh kg^{-1}) was calculated using the following equation:

$$E = i\,\Delta V \mathrm{d}t/m \tag{2}$$

where m represents the mass of the active material, ΔV the cell voltage during discharge and i the current. The specific power (W kg^{-1}) stored by the supercapacitor is obtained by dividing the energy by the discharge time t:

$$P = E/t \tag{3}$$

The higher energy density reached for a PANCF–PANI supercapacitor is 4.25 Wh kg^{-1}. The power density computed from the data of Figure 8 is 1.2 kW kg^{-1} for a discharge time of 13 s. Higher values could easily be reached by increasing the potential range in which the electrodes are cycled. Attention should be directed to the optimization of the potential range in the future. This is important since, for example, values as high as 5.8 Wh kg^{-1} and 1500 W kg^{-1} are reached for

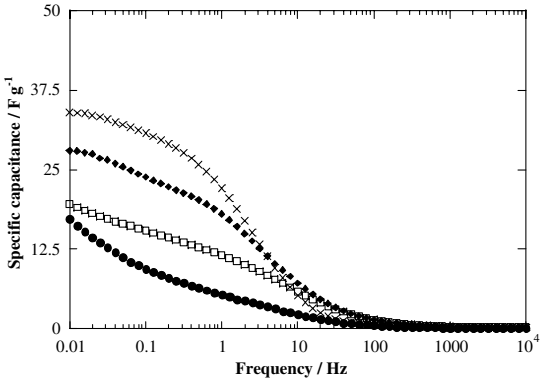

Fig. 12. Frequency dependence of the specific capacitance for different PANI onto PAN aerogel deposition times in 2-symmetrical supercapacitor geometry. Key: (●) 2, (□) 5, (♦) 10 and (×) 20 s.

the sample obtained with a deposition time of 35 s when cycled over 0.8 V, that is 1.4 times higher than values reported when cycled up to 0.6 V. Oxygen in solution should also be taken into account, an efficient O_2 removal from solution being essential. The short-range goals established by the US Department of Energy (DOE) for electric vehicle power supercapacitors ($E > 5$ Wh kg^{-1}, $P > 500$ W kg^{-1}) can be reached by a PANCF–PANI based supercapacitor device by increasing the cycle potential range, even if it remains clear that additional work is required to improve the stability of PANCF–PANI capacitors in a larger potential range ($\Delta V > 0.6$ V) and maintain the initial discharge capacity. Values reached with this PANI–PANCF system are higher than those previously reported for a PANI system [17].

4. Conclusion

Galvanostatic charge–discharge cycling experiments indicate an energy density of about 429 Wh kg^{-1} for the active material with a power density of 12 kW kg^{-1} for a 13 s discharge time. Energy and power densities should be increased by a factor of 1.4 to 1.7 by enlarging the potential range in which the electrodes are cycled. After a decrease during the first few cycles, the discharge capacity remains constant.

Polyaniline can be oxidized to a p-type polycation but its reduction leads to an isolating neutral state which limits the power achievable with this material as a pseudocapacitor electrode. The supercapacitor performances may be optimized further by the choice of an other conducting polymer which can be p and n-doped, on the surface of the PAN aerogel electrode, or by the use of two different polymers, one p-doped as the anode (like polyaniline) and a n-doping polymer (like poly(3-methythiophene)) as the cathode. The electrochemical behaviour of such a supercapacitor and its feasibility as an electrochemical capacitor will be discussed in a following paper.

Acknowledgements

This work was supported by an NSERC (strategic grant). H.T. is grateful to INRS for an INRS postdoctoral fellowship.

References

1. C. Nui, E.K. Sichel, R. Hoch, D. Moy and H. Tennet, *Appl. Phys. Lett.* **70** (1997) 1480.
2. B.E. Conway, 'Electrochemical Supercapacitors: Scientific Fundamentals and Technological Applications' (Academic/Plenum, New York, 1999).
3. B.E. Conway, *J. Electrochem. Soc.* **138** (1991) 1539.
4. P. Gouérec, D. Miousse, F. Tran-Van and L.H. Dao, *J. New Mater. Electrochem. Syst.* **2** (1999) 221.
5. P. Gouérec, H. Talbi, D. Miousse, F. Tran-Van, K.H. Lee and L.H. Dao, *J. Electrochem. Soc.* **148** (2001) 94.
6. C. Arbizzani, M. Mastragostino, L. Meneghello and R. Paraventi, *Adv. Mater.* **8** (1996) 331.
7. A. Rudge, J. Davey, I. Raistrick, S. Gottesfeld and J.P. Ferraris, *J. Power Sources* **47** (1994) 89.
8. J.C. Chiang and A.G. Mac Diarmid, *Synth. Met.* **13** (1986) 193.
9. A.G. MacDiarmid, L.S. Yang, W.S. Huang and B.D. Humphrey, *Synth. Met.* **18** (1987) 393.
10. L-S. Yang, Z-Q. Shan and Y-L. Liu, *J. Power Sources* **34** (1991) 141.
11. L. Yang, W. Qiu and Q. Liu, *Solid State Ionics* **86** (1996) 819.
12. P. Novak, K. Muller, K.S.V. Santhanam and O. Haas, *Chem. Rev.* **97** (1997) 207.
13. M. Morita, S. Miyazaki, M. Ishikawa, Y. Matsuda, H. Tajima, K. Adachi and F. Anan, *J. Electrochem. Soc.* **142** (1995) 3.
14. J. Desilvestro, W. Scheifele and O. Haas, *J. Electrochem. Soc.* **139** (1992) 2727.
15. J.P. Zheng, J. Huang and T.R. Jow, *J. Electrochem. Soc.* **144** (1997) 2026.
16. B. Garcia, F. Fusalba and D. Bélanger, *Can. J. Chem.* **75** (1997) 1536.
17. D. Belanger, X.M. Ren, J. Davey, F. Uribe and S. Gottesfeld, *J. Electrochem. Soc.* **147** (2000) 2923.
18. A. Dang, D. Miousse, H. Talbi and L.H. Dao, in preparation.
19. S. Yonezawa, K. Kanamura and Z-I. Takehara, *J. Electrochem. Soc.* **140** (1993) 629.
20. S. Yonezawa, K. Kanamura and Z-I. Takehara, *J. Electrochem. Soc.* **142** (1995) 3309.
21. S.H. Jordanov, H.A. Kozlowska and B.E. Conway, *J. Electrochem. Soc.* **125** (1978) 1471.
22. D. Qu and H. Shi, *J. Power Sources* **74** (1998) 99.
23. S.T. Mayer, R.W. Pekala and J.L. Kaschmitter, *J. Electrochem. Soc.* **140** (1993) 2.
24. H. Talbi, A. Dang, L.H. Dao and K.H. Lee, submitted for publication in *J. Appl. Chem.*
25. A.A. Pud, *Synth. Met.* **66** (1994) 1.
26. H.N. Dinh, J. Ding, S.J. Xia and V.I. Birss, *J. Electroanal. Chem.* **459** (1998) 45.
27. F. Fusalba, N.E. Mehdi, L. Breau and D. Bélanger, *Chem. Mater.* **11** (1999) 2743.
28. C. Arbizzani, M. Mastragostino and L. Meneghello, *Electrochim. Acta* **40** (1995) 2223.
29. M. Schwarzenberg, K. Jobst and L. Sawtschenko, *Electrochim. Acta* **35** (1990) 403.
30. A. Laforgue, P. Simon, C. Sarrazin and J-F. Fauvarque, *J. Power Sources* **80** (1999) 142.
31. B.E. Conway, *J. Power Sources* **63** (1996) 255.